The effectiveness of emg-driven neuromusculoskeletal model calibration is task dependent

THE EFFECTIVENESS OF EMG-DRIVEN NEUROMUSCULOSKELETAL MODEL CALIBRATION IS TASK DEPENDENT

Azadeh Kian[1], Claudio Pizzolato[2], Mark Halaki[3], Karen Ginn[4],
David Lloyd[2], Darren Reed[4], David Ackland[1]

[1]Department of Biomedical Engineering, University of Melbourne, Australia

[2] Griffith Centre of Biomedical and Rehabilitation Engineering, Menzies Health Institute Queensland and School of Allied Health Sciences, Griffith University, Australia

[3]Discipline of Exercise and Sport Science, Sydney School of Health Sciences, Faculty of Medicine and Health, The University of Sydney

[4]Discipline of Anatomy & Histology,
Faculty of Medicine and Health, The University of Sydney

Submitted as a Short Communication to

Journal of Biomechanics

Word count (Introduction to Discussion): 1,684

Address for correspondence:
David C. Ackland
Department of Biomedical Engineering
University of Melbourne
Parkville, Victoria 3010, AUSTRALIA
Phone: +613 8344 0405
Fax: +613 9347 8784

Keywords: electromyography; shoulder; biomechanical model; rotator cuff; deltoid; static optimization

ABSTRACT

Calibration of neuromusculoskeletal models using functional tasks is performed to calculate subject-specific musculotendon parameters, as well as coefficients describing the shape of muscle excitation and activation functions. The objective of the present study was to employ a neuromusculoskeletal model of the shoulder driven entirely from muscle electromyography (EMG) to quantify the influence of different model calibration strategies on muscle and joint force predictions. Three healthy adults performed dynamic shoulder abduction and flexion, followed by calibration tasks that included reaching, head touching as well as active and passive abduction, flexion and axial rotation, and submaximal isometric abduction, flexion and axial rotation contractions. EMG data were simultaneously measured from 16 shoulder muscles using surface and intramuscular electrodes, and joint motion evaluated using video motion analysis. Muscle and joint forces were calculated using subject-specific EMG-driven neuromusculoskeletal models that were uncalibrated and calibrated using (i) all calibration tasks (ii) sagittal plane calibration tasks (iii) scapular plane calibration tasks. Joint forces were compared to published instrumented implant data. Calibrating models across all tasks resulted in glenohumeral joint force magnitudes that were more similar to instrumented implant data than those derived from any other model calibration strategy. Muscles that generated greater torque were more sensitive to calibration than those that contributed less. This study demonstrates that extensive model calibration over a broad range of contrasting tasks produces the most accurate and physiologically relevant musculotendon and EMG-to-activation parameters. This study will assist in development and deployment of subject-specific neuromusculoskeletal models.

INTRODUCTION

The evaluation of musculotendon parameters, as well as coefficients describing the shape of the muscle excitation and activation functions, presents a challenge in EMG-driven neuromusculoskeletal modelling. These values must be estimated using a calibration process that matches model estimates of net joint moments to those calculated directly from inverse dynamics over a specific set of tasks. At the shoulder, musculotendon calibration has been achieved using isometric contractions and dynamic joint motion including activities of daily living (Kian et al., 2019, Assila et al., 2020). However, the dependence of the chosen calibration tasks on neuromusculoskeletal model estimates of muscle and joint loading remain poorly understood, and the chosen calibration tasks are known to be a significant source of model output variability. The aim of this study was to employ an EMG-driven neuromusculoskeletal model of the shoulder to quantify the influence of model calibration tasks on muscle and joint force predictions. The findings will have implications for development and deployment of EMG-driven and EMG-informed neuromusculoskeletal models.

MATERIALS AND METHODS

Subject recruitment and testing

Three healthy female adults with no history of upper limb pain, disease or previous surgery were recruited for testing (mean age: 23.7±6.4 years; body mass: 55.7±3.2 kg; height: 165.0±2.6 cm). Testing followed a previously published protocol and is only briefly described here (Kian et al., 2019). The participants performed dynamic shoulder movements while standing which included shoulder abduction and flexion at a rate of 60° per second. The participants then performed three sets of calibration tasks comprising general movements, and sagittal plane and scapular plane tasks, which were chosen because they span different mechanical degrees of freedom (DOF) at the shoulder. The general calibration movements were reaching, head touching and submaximal isometric internal and external rotation of the shoulder with the arm in 90° of abduction and the elbow flexed to 90°, while the sagittal plane tasks incorporated (i) active flexion of the shoulder at approximately 30° per second with the elbow extended, (ii) passive flexion of the shoulder, and (iii) sub-maximal isometric flexion and extension of the shoulder with the arm in 90° of flexion. The scapular plane tasks consisted of (i) abduction at approximately 30° per second with the elbow extended, (ii) passive abduction of the shoulder, and (iii) sub-maximal isometric abduction and adduction of the shoulder with the arm in 90° of abduction. All isometric contractions were performed using an instrumented handle and consisted of four seconds of gradual load increase to 50% maximal effort, three seconds of sustained contraction at 50% maximal effort, followed by four seconds of load decrease to resting level. Subjects followed a visual trajectory of their contraction on a monitor to guide their contraction execution. Ethical approval was obtained through the University of Sydney Human Research Ethics Committees, and participants provided written informed consent.

During testing, pairs of surface EMG electrodes (Red Dot, 2258, 3M) were placed over pectoralis major, upper trapezius, lower trapezius, biceps brachii and triceps brachii. Bipolar intramuscular (in-dwelling) electrodes were placed in anterior, middle and posterior deltoid sub-regions, rhomboid major, supraspinatus, infraspinatus, subscapularis, pectoralis minor, serratus anterior, teres major, and latissimus dorsi (Boettcher et al., 2008, Johnson et al., 2011, Ginn and Halaki, 2015), with ultrasonic guidance employed for rhomboid major and pectoralis minor electrode placement (Mindray, DP-9900). Upper limb joint kinematics was simultaneously recorded during testing using a 4-camera video motion analysis system (Vicon, UK). The trajectories of 15 retroreflective markers placed on the upper-limb were digitised and inverse kinematics employed to calculate joint angles (Wu et al., 2016).

Musculoskeletal modelling

EMG-driven neuromusculoskeletal model of each participant were created as described previously (Kian et al., 2019). Each model comprised 5-segments and 10 degree-of-freedom. The glenohumeral and acromioclavicular joints were modeled as 3-degree-of-freedom ball and socket joints, and the sternoclavicular and elbow joints as 2-degree-of-freedom universal joints. The joints were actuated by 23 Hill-type musculotendon units, which comprised 5 axiohumeral, 10 axioscapular and 8 scapulohumeral muscles and muscle sub-regions. Each muscle's neural excitation was calculated from its pre-processed EMG signal using a second order linear differential equation cast as a numerical backward differences formula:

$$u(t) = \alpha e(t-d) - (C_1 + C_2)u(t-1) - C_1.C_2u(t-2)$$

Equation 1

where $e(t)$ is the time-varying muscle excitation, $u(t)$ the neural excitation, d the electromechanical delay, α a muscle gain coefficient, and C_1 and C_2 recursive coefficients (Lloyd and Besier, 2003). Muscle activation was modeled using a non-linear neural excitation function (Lloyd and Besier, 2003):

$$a(t) = \frac{e^{A.u(t)} - 1}{e^{A} - 1}$$

Equation 2

where $a(t)$ is the time-varying muscle activation, $u(t)$ the time-varying neural excitation and A, a non-linear shape factor ranging between zero (a straight-line) and 3 (highly non-linear). Muscle forces were subsequently calculated using a Hill-type model of each musculotendon actuator:

$$F^{m}(t) = F^{t}(t) = F^{max}\left[f_a(l_m).f_v(v_m).a(t) + f_p(l_m) + d_m.v_m\right].\cos\varphi$$

Equation 3

where $F^m(t)$ is the time-varying force generated by the sum of muscle fibers, F^t the tendon force, F^{max} the maximum isometric muscle force, $f_a(l_m)$ the active force-length relation, $f_v(v_m)$ the muscle fibre contraction velocity relation, $f_p(l_m)$ the passive force- length relation, d_m a muscle damping coefficient, and φ the muscle pennation angle.

The muscle-tendon parameters consisted of optimum muscle fibre length, l_o^m, tendon slack length, l_s^t, and maximum isometric muscle force, F_o^m, as well as the EMG-to-activation coefficients (C_1, C_2 and A). These parameters were calibrated for each subject using three strategies: (i) all calibration tasks (ii) sagittal plane calibration tasks, and (iii) scapula plane calibration tasks. In addition, the 'uncalibrated' model was also employed where generic values for l_o^m, l_s^t, and F_o^m were taken directly from the scaled musculoskeletal model, and default values of *C1, C2* and *A* were adopted (0.5, -0.5, and 0.1, respectively). Using the four models produced by each calibration strategy, muscle and joint contact forces calculated for abduction and flexion were computed, and joint force compared to published instrumented implant data (Nikooyan et al., 2010, Bergmann et al., 2007). Specifically, data reported by Nikooyan et al. (2010) from two instrumented shoulder implant recipients following hemi-arthroplasty (referred to as 'implant 1' and 'implant 2', respectively) for the treatment of osteoarthritis without rotator cuff damage (Table 1). The joint replacement procedures were performed using a deltopectoral approach, and joint force data were obtained seven and ten months post-operatively for implant 1 and 2, respectively.

RESULTS

EMG-driven neuromusculoskeletal model calibration strategy had a substantial influence on calculated glenohumeral joint forces for the dynamic shoulder tests (Fig. 1 and Table 2). Calibrating models across all tasks resulted in calculated glenohumeral joint force magnitudes that were more similar to instrumented implant data than those derived from any other model calibration strategy. Specifically, the RMS difference between calculated and measured glenohumeral joint force during abduction was 7.1%BW for implant 1 and 10.8%BW for implant 2 (Table 3).

Calibrating the neuromusculoskeletal model using sagittal plane tasks resulted in joint force results that were of similar magnitude to those when the model was calibrated using all tasks. For example, during abduction, the RMS difference between calculated and measured glenohumeral joint force was 8.0%BW and 15.2%BW for implant 1 and 2, respectively. In contrast, calibrating the neuromusculoskeletal model using scapular plane tasks resulted in more substantial differences between calculated and measured glenohumeral joint force, for instance, during abduction the RMS differences between calculated and measured glenohumeral joint force was 13.3%BW and 23.0%BW for implant 1 and 2, respectively. The uncalibrated model resulted in the largest differences between calculated and measured glenohumeral joint force. During abduction, for example, the RMS differences between calculated and measured glenohumeral joint force was 39.9%BW and 55.6%BW for implant 1 and 2, respectively."

The middle deltoid, pectoralis major and latissimus dorsi had notably higher muscle forces calculated using the uncalibrated model during abduction (Fig. 2) and flexion (Fig. 3) compared to those calculated using the calibrated models. For these muscles, calibrating the model across all tasks or tasks in one given plane produced similar overall muscle force trends. A neuromusculoskeletal model calibrated across all tasks tended to produce lower muscle forces than that calibrated in the scapular or sagittal plane or when an uncalibrated model was employed.

DISCUSSION

The present study showed that calibrating EMG-driven neuromusculoskeletal models across a broad range of tasks in multiple planes produced glenohumeral joint forces that were more similar to those measured in instrumented implants than when the models were calibrated only in one plane, or not calibrated at all. Even glenohumeral joint forces computed during abduction using a model calibrated exclusively with tasks in this elevation plane exhibited greater discrepancy with instrumented implant data. The results also demonstrate that net joint moments calculated from neuromusculoskeletal models calibrated across a broad range of tasks were more similar to joint moments calculated from inverse dynamics than when the models were calibrated in one plane or not calibrated at all (see Table 4). These findings suggest that neuromusculoskeletal models that are more extensively calibrated across broad and contrasting tasks produced more physiologically plausible and broadly applicable musculotendon and EMG-to-activation model parameters, and therefore, the most accurate the estimates of muscle and joint loading.

When considering data for individual subjects, the results show that model calibration in one plane may in some cases be inadequate and lead to net joint moments and joint forces that are less accurate those than in the case of the uncalibrated model (see Supplementary Material). For example, the RMS difference between the net abduction joint moment and the corresponding inverse dynamics joint moment for subject 1 was 0.22%BWm, 0.86%BWm, 1.15%BWm and 0.60%BWm when the model was calibrated using all tasks, calibrated using sagittal plane tasks, calibrated using scapular plane tasks, and not calibrated, respectively. This finding further reinforces the importance of rigorous model calibration across diverse tasks in contrasting motion planes.

EMG-driven neuromusculoskeletal model calibration, compared to no calibration, had a substantial impact on the force estimates of prime mover muscles, which included the middle deltoid, pectoralis major and latissimus dorsi, though the force estimates of these muscles were not discernibly different between calibration methods. For a number of other muscles such as the anterior deltoid, posterior deltoid, supraspinatus and subscapularis, calibration method substantially affected calculated muscle forces during abduction and flexion, reflecting greater sensitivity of muscle activation to calibration task. These findings largely reflect the changes in parameters that occurred during model calibration. The calibration algorithm, for instance, was tuned to have greater weighting on a muscle's maximum isometric force, F_o^m, than tendon slack length, l_s^t, which has been shown to have proportionally less variance in healthy cohorts (Wu et al., 2016).

This study has some limitations. First, model calibration was primarily across the glenohumeral joint, and different results may occur if the calibration trials explicitly incorporated the elbow, or multiple DOF across both joints. There are other forms of EMG-informed neuromusculoskeletal models, and this study examined EMG-driven models in which all muscles in the model had corresponding EMGs. Calibrated EMG-hybrid models, for instance, also incorporate excitations that are estimated for muscles without recorded EMGs. Nevertheless, in such models we would still expect the contrasting calibration tasks across multiple DOF to improve tracking between excitations and EMGs and joint contact force estimates. Finally, our analysis focused on three test subjects, and this study was therefore not powered for statistical analysis. Nonetheless, this study observed strong trends across all subjects that were used to derive the study conclusions, including differences in computed muscle and joint forces with neuromusculoskeletal model calibration strategy. The consistent patterns of within subject differences in model calibration strategy observed suggests the findings may be generalizable to other subject cohorts.

In conclusion, this study demonstrated that extensive model calibration over a broad range of contrasting tasks is required to achieve the most physiologically plausible and broadly applicable musculotendon and EMG-to-activation parameters in EMG-driven neuromusculoskeletal modelling. Quality of model calibration affects muscle forces in a task-dependent manner. The findings of this study will assist in development and deployment of EMG-driven and EMG-informed neuromusculoskeletal models in the estimation of muscle and joint loading.

ACKNOWLEDGMENTS

This research was supported by an Australian Research Council Future Fellowship to D.C.A (FT200100098).

REFERENCES

ASSILA, N., PIZZOLATO, C., MARTINEZ, R., LLOYD, D. G. & BEGON, M. 2020. EMG-Assisted Algorithm to Account for Shoulder Muscles Co-Contraction in Overhead Manual Handling. *Applied Sciences,* 10, 3522.

BERGMANN, G., GRAICHEN, F., BENDER, A., KÄÄB, M., ROHLMANN, A. & WESTERHOFF, P. 2007. In vivo glenohumeral contact forces—measurements in the first patient 7 months postoperatively. *Journal of Biomechanics,* 40, 2139-2149.

BOETTCHER, C. E., GINN, K. A. & CATHERS, I. 2008. Standard maximum isometric voluntary contraction tests for normalizing shoulder muscle EMG. *Journal of Orthopaedic Research,* 26, 1591-1597.

GINN, K. A. & HALAKI, M. 2015. Do surface electrode recordings validly represent latissimus dorsi activation patterns during shoulder tasks? *Journal of Electromyography and Kinesiology,* 25, 8-13.

JOHNSON, V. L., HALAKI, M. & GINN, K. A. 2011. The use of surface electrodes to record infraspinatus activity is not valid at low infraspinatus activation levels. *Journal of Electromyography and Kinesiology,* 21, 112-118.

KIAN, A., PIZZOLATO, C., HALAKI, M., GINN, K., LLOYD, D., REED, D. & ACKLAND, D. 2019. Static optimization underestimates antagonist muscle activity at the glenohumeral joint: A musculoskeletal modeling study. *Journal of Biomechanics,* 97, 109348.

LLOYD, D. G. & BESIER, T. F. 2003. An EMG-driven musculoskeletal model to estimate muscle forces and knee joint moments in vivo. *Journal of Biomechanics,* 36, 765-776.

NIKOOYAN, A., VEEGER, H., WESTERHOFF, P., GRAICHEN, F., BERGMANN, G. & VAN DER HELM, F. 2010. Validation of the Delft Shoulder and Elbow Model using in-vivo glenohumeral joint contact forces. *Journal of Biomechanics,* 43, 3007-3014.

PIZZOLATO, C., LLOYD, D. G., SARTORI, M., CESERACCIU, E., BESIER, T. F., FREGLY, B. J. & REGGIANI, M. 2015. CEINMS: A toolbox to investigate the influence of different neural control solutions on the prediction of muscle excitation and joint moments during dynamic motor tasks. *Journal of Biomechanics,* 48, 3929-3936.

WU, W., LEE, P. V., BRYANT, A. L., GALEA, M. & ACKLAND, D. C. 2016. Subject-specific musculoskeletal modeling in the evaluation of shoulder muscle and joint function. *Journal of Biomechanics,* 49, 3626-3634.

FIGURE CAPTIONS

Fig. 1. Mean glenohumeral joint force across all subjects (%BW) estimated using the EMG-driven neuromusculoskeletal model for abduction (A) and flexion (B). Shown are results when musculotendon parameters were calibrated using all tasks (solid black line), tasks in the sagittal plane (dash dotted), tasks in the scapular plane (dotted) and in the case of a model with musculotendon parameters that were not calibrated (triangles). *In vivo* glenohumeral joint forces are given for Nikooyan et al., 2010 subject 1 (dashed red line) and subject 2 (dotted red line)

Fig. 2. Mean muscle forces across all subjects (%BW) estimated using the EMG-driven neuromusculoskeletal model during scapular-plane abduction. Shown are results when musculotendon parameters were calibrated using all tasks (solid line), tasks in the sagittal plane (dash dotted), tasks in the scapular plane (dotted), and in the case of a model with musculotendon parameters that were not calibrated (dashed). Data are given for nine selected muscles spanning the glenohumeral joint including the anterior deltoid (DeltA), middle deltoid (DeltM), posterior deltoid (DeltP), supraspinatus (Supra), infraspinatus (Infra), subscapularis (Subs), pectoralis major (PMaj), latissimus dorsi (LDorsi) and teres major (TMaj).

Fig. 3. Mean muscle forces across all subjects estimated using the EMG-driven neuromusculoskeletal model during flexion. Given are results when musculotendon parameters were calibrated using all tasks (solid line), tasks in the sagittal plane (dash dotted), tasks in the scapular plane (dotted), and in the case of a model with musculotendon parameters that were not calibrated

(dashed). Data are given for nine selected muscles spanning the glenohumeral joint. For muscle definitions see caption of Figure 2.

Figure 1

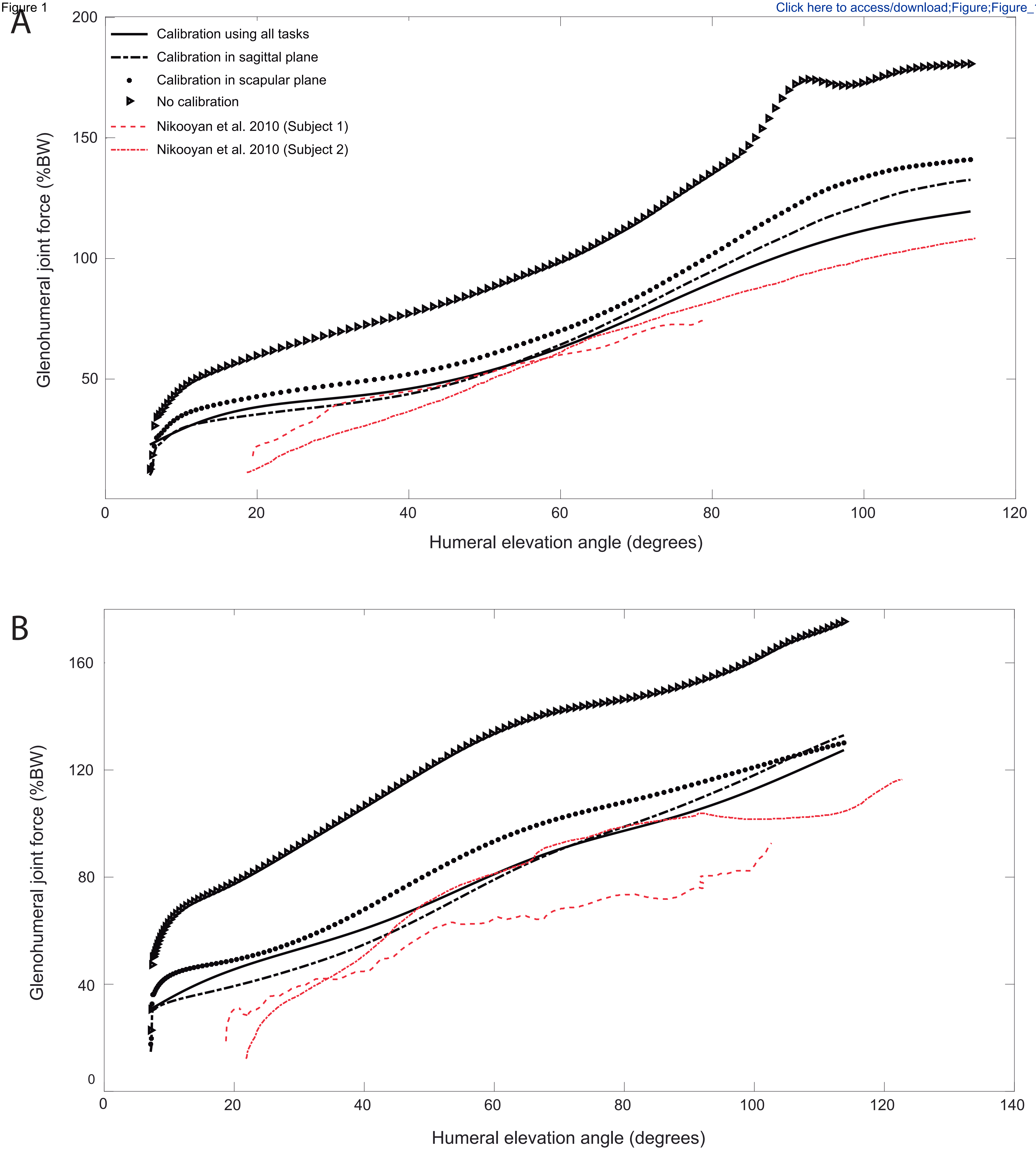
A
Calibration using all tasks
Calibration in sagittal plane
Calibration in scapular plane
No calibration
Nikooyan et al. 2010 (Subject 1)
Nikooyan et al. 2010 (Subject 2)
Glenohumeral joint force (%BW)
Humeral elevation angle (degrees)
0
20
40
60
80
100
120
50
100
150
200
B
Glenohumeral joint force (%BW)
Humeral elevation angle (degrees)
0
20
40
60
80
100
120
140
40
80
120
160

Figure 2

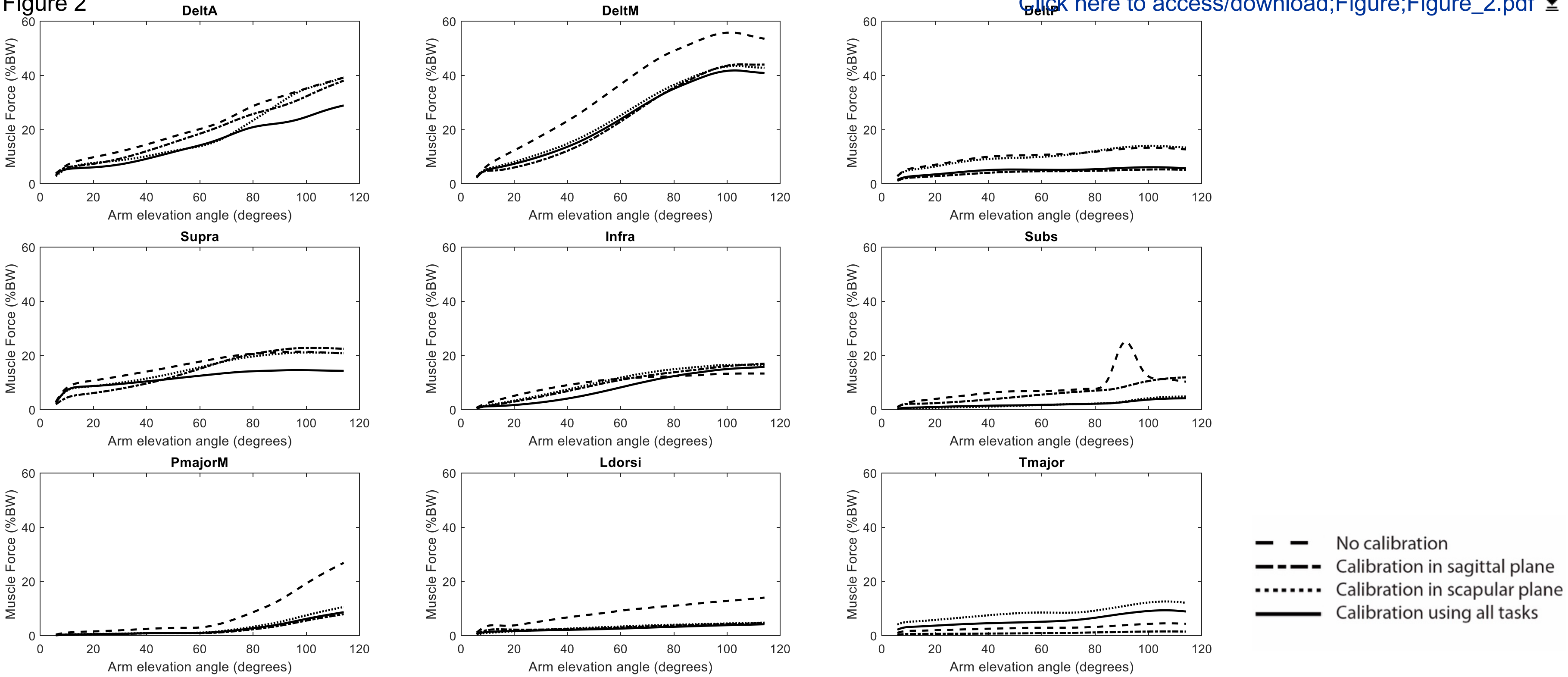
DeltA
DeltM
DeltP
Supra
Infra
Subs
PmajorM
Ldorsi
Tmajor
Muscle Force (%BW)
Arm elevation angle (degrees)
No calibration
Calibration in sagittal plane
Calibration in scapular plane
Calibration using all tasks

Figure 3

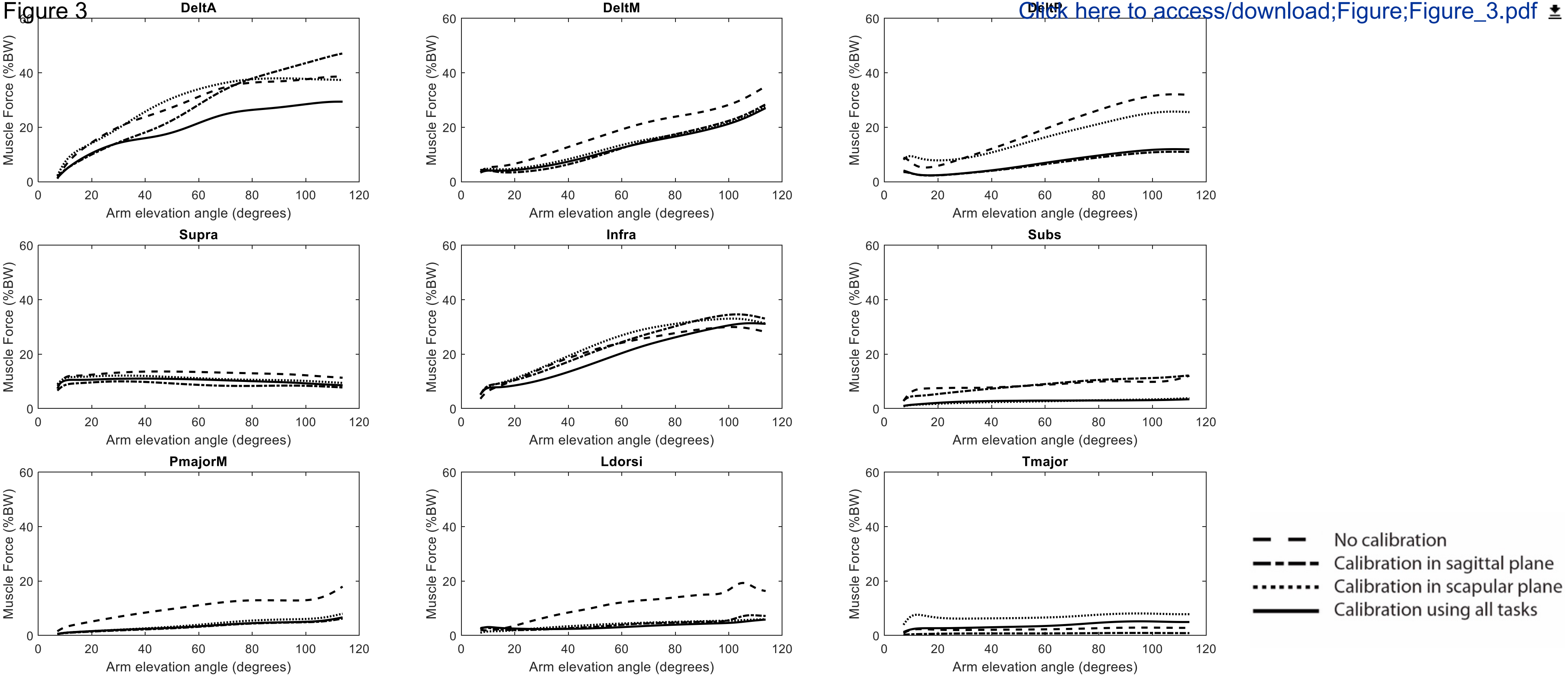
DeltA
DeltM
DeltP
Supra
Infra
Subs
PmajorM
Ldorsi
Tmajor
Muscle Force (%BW)
Arm elevation angle (degrees)
No calibration
Calibration in sagittal plane
Calibration in scapular plane
Calibration using all tasks

Table 1: Demographic data for participants in the current study. Instrumented implant data previously reported by Nikooyan et al. 2010 are indicated with an asterisk.

	Sex	**Age (yrs)**	**Height (cm)**	**Weight(kg)**	**BMI (kg/m^2)**	**Side**
Subject 1	Female	31	164	57	21.2	Right
Subject 2	Female	19	168	52	18.4	Right
Subject 3	Female	21	163	58	21.8	Right
Implant 1*	Female	73	168	72	25.5	Left
Implant 2*	Male	64	163	85	32	Right

Table 2: Mean and standard deviation (SD) data for glenohumeral joint force magnitude (%BW) calculated using an EMG-driven neuromusculoskeletal model. Data are provided for the model when calibrated using all tasks, calibrated in the sagittal plane and scapular plane, and when not calibrated. Given are results for shoulder abduction in the scapular plane and flexion in the sagittal plane.

	Abduction						**Flexion**					
	30 degrees		60 degrees		90 degrees		30 degrees		60 degrees		90 degrees	
	Mean	SD	Mean	SD	Mean	SD	Mean	SD	Mean	SD	Mean	SD
Calibration using all tasks	41.9	4.0	63.7	25.4	102.3	54.4	53.7	11.9	81.7	19.4	104.4	37.0
Calibration in sagittal plane	39.0	7.2	65.0	36.5	109.8	67.3	46.8	6.4	79.8	26.6	108.1	43.0
Calibration in scapular plane	47.4	8.9	70.7	20.3	120.4	61.1	57.3	18.3	94.0	31.8	114.4	45.0
No model calibration	68.8	9.1	99.8	23.1	169.9	29.0	93.2	8.9	134.7	19.9	152.4	24.3

Table 3: RMS differences in glenohumeral joint force magnitude (%BW) estimated between the EMG-driven neuromusculoskeletal model and *in vivo* instrumented implant measurements reported by Nikooyan et al., (2010) for two subjects, denoted implant 1 and implant 2. Data are provided for the model when calibrated using all tasks, calibrated in the sagittal plane and scapular plane, and when not calibrated. Given are results for shoulder abduction in the scapular plane and flexion in the sagittal plane.

	Abduction		Flexion	
	Implant 1	Implant 2	Implant 1	Implant 2
Calibration using all tasks	7.1	10.8	20.4	11.7
Calibration in sagittal plane	8.0	15.2	20.8	12.0
Calibration in scapular plane	13.2	23.0	28.8	16.9
No model calibration	39.9	55.6	67.1	55.4

Table 4: RMS differences in net glenohumeral joint moments (%BW.m) between the EMG-driven neuromusculoskeletal model calculations and those computed directly using inverse dynamics. Data are provided for the model when calibrated using all tasks, calibrated in the sagittal plane and scapular plane, and when not calibrated. Given are results for shoulder abduction in the scapular plane and flexion in the sagittal plane.

	Abduction	Flexion
Calibration using all tasks	0.14	0.09
Calibration in sagittal plane	0.17	0.16
Calibration in scapular plane	0.20	0.17
No model calibration	0.47	0.28